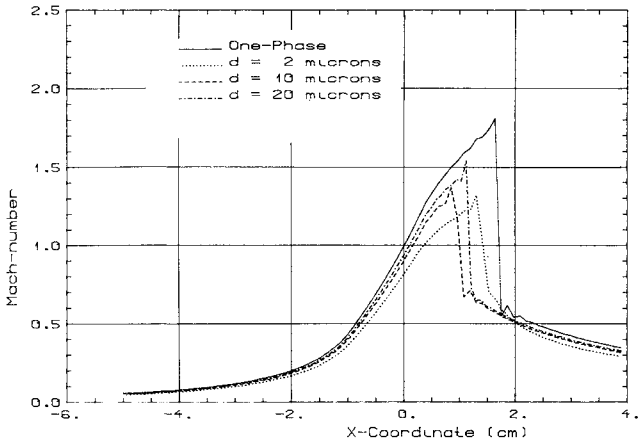

Fig. 4 Gas Mach number distribution (loading ratio of 0.429).

In order to calculate the critical velocity of sound in the suspension, the slip ratio is

$$S = 1 - w/b \tag{17}$$

where $w = u_g - u_p$.

For quasi-gas calculation, the critical condition occurs at the minimum cross-sectional area. The quasi-gas Mach number M_Q is

$$M_Q = M_g(c/b) \tag{18}$$

Using Eqs. (16-18) with the condition in Fig. 3 gives the quasi-gas Mach number $M_Q = 1$, i.e., shocked flow in the nozzle. Furthermore, this implies that the gas/particle mixture can have a region with supersonic (quasi-gas supersonic) flow and, in order to satisfy a given back pressure, a mixture-shock will occur.

Figure 4 shows the Mach number distribution in the nozzle for loading ratio 0.429 and particle diam 2, 10, and 20 μm. The figure shows that the strength of the frozen shock increases with increased particle diameters. The location of the shock has a more complicated pattern. At first the shock location moves upstream and then downstream for increased particle diameters. This can be explained using physics. The smaller particles have more influence on the gas flow for the same particle loading. This is due to the fact that, for the same particle loading, the total particle surface area effective for momentum and energy exchange between gas and particles is greater in a two-phase flowfield involving smaller diameter particles. The diameter of the particles will then have influence on the flow upstream of the shock, the frozen shock, and the relaxation zone behind the frozen shock. In order to satisfy a given back pressure, the location of the frozen shock will move upstream and downstream dependent of the upstream condition, the pressure rise in the frozen shock, in the relaxation zone, and due to the cross-sectional area change.

Conclusions

Quasi-one-dimensional gas/particle flows with shock inside a nozzle have been studied numerically herein. The results show: 1) the complexity of the shock pattern is dependent on loading ratio and particle diameter and 2) the strength of the shock is influenced stongly by the presence of the particles. The study also shows the mixture-shock condition in the gas/particle nozzle flow, caused by the fact that the velocity of sound for the gas/particle mixture is less than the velocity of sound for the gas phase, and the quasi-gas Mach number is above one.

References

[1]Rudinger, G., "Flow of Solid Particles in Gases," AGARDograph No. 222, 1976.

[2]Rudinger, G., "Some Effects on Finite Particle Volume on the Dynamics of Gas-Particle Mixtures," *AIAA Journal*, Vol. 3, July 1965, pp. 1217-1222.

[3]Kriebel, A. R., "Analysis of Normal Shock Waves in Particle Laden Gas," *Transactions of ASME, Journal of Basic Engineering*, Dec. 1964, pp. 655-665.

[4]Zucrow and Hoffmann, *Gas Dynamics*, Vol. II, John Wiley & Sons, Inc., New York, 1977, pp. 53-67.

[5]Wallis, G. B., "One-Dimensional Two-Phase Flow," McGraw-Hill Book Co., New York, 1969.

[6]Di Giacinto, M., Sabetta, F., and Piva, R., "Two-Way Coupling Effects in Dilute Gas-Particle Flows," *Transactions of ASME Journal of Fluids Engineering*, Vol. 104, Sept. 1982, pp. 304-312.

[7]Chang, I.-S., "One- and Two-Phase Nozzle Flows," *AIAA Journal*, Vol. 18, Dec. 1980, pp. 1455-1461.

[8]Sharma, M. P. and Crowe, C. T., "A Novel Physico-Computational Model of Quasi One-Dimensional Gas-Particle Flows," *Transactions of ASME, Journal of Fluids Engineering*, Vol. 100, Sept. 1978, pp. 343-349.

[9]Chang, I.-S., "Three-Dimensional, Two-Phase Supersonic Nozzle Flows," *AIAA Journal*, Vol. 21, May 1983, pp. 671-678.

[10]Rudinger, G., "Some Properties of Shock Relaxation in Gas Flows Carrying Small Particles," *The Physics of Fluids*, Vol. 7, May 1964, pp. 658-663.

[11]Carlson, D. J. and Høglund, R. F., "Particle Drag and Heat Transfer in Rocket Nozzles," *AIAA Journal*, Vol. 2, Nov. 1964, pp. 1980-1984.

[12]Cuffel, R. F., Back, L. H., and Massier, P. F., "Transonic Flowfield in a Supersonic Nozzle with Small Throat Radius of Curvature," *AIAA Journal*, Vol. 7, July 1968, pp. 1364-1366.

[13]Førde, M., "Velocity of Sound in Non-Equilibrium Gas/Particle Flows," Division of Aero- and Gas-Dynamics, NTH Trondheim, Norway, Rept. IFAG-A-159, 1984.

Surface Renewal Model for Turbulent Boundary-Layer Flow

L. C. Thomas* and K. F. Loughlin†
University of Petroleum and Minerals
Dhahran, Saudi Arabia

Introduction

THE standard approach to characterizing the wall region for turbulent boundary-layer flow involves the use of the van Driest[1] damping factor relationship for mixing length ℓ

$$\ell^+ = \kappa y^+ [1 - \exp(-y^+/a^+)] \tag{1}$$

where κ is an empirical constant and a^+ is associated with the dimensionless frequency of idealized fluid oscillations near the wall; κ is generally set equal to 0.41 and a^+ is specified by empirical correlations. However, the damping factor approach has not been found to provide a secure basis for generalization. For example, the damping factor approach has been of limited value in characterizing transitional turbulent flow and variable property flows. Furthermore, damping factor formulations for eddy thermal conductivity (or turbulent Prandtl number, Pr_t) appear to have

Received Dec. 4, 1984; revision received Aug. 26, 1985.

*Professor, Department of Mechanical Engineering.
†Associate Professor, Department of Chemical Engineering.

inconsistencies and are seldom used in analyzing turbulent convection heat transfer. This lack of generality in the damping factor approach appears to be partly due to the artificial wall/fluid perspective upon which it is based.

An alternative approach to analyzing wall turbulence has been developed over the past few years. In this surface renewal approach, the turbulent transport within the large-scale coherent constant structures associated with the turbulent burst phenomenon is modeled. Similar to the damping factor method, this model treats wall turbulence as an unsteady transport process. However, in this approach the fluid is taken as the fluctuating medium with the relative velocity of the fluid at the wall appropriately set equal to zero, and the contribution of the unsteady fluctuating velocity to the mean velocity is accounted for statistically. Because of its more realistic theoretical basis, the surface renewal modeling approach appears to provide a better basis for generalization than the damping factor approach.

In this Note, the elementary surface renewal model is coupled with the classical mixing-length representation of the turbulent core to develop an inner law for fully turbulent boundary-layer flow with adverse and favorable pressure gradients. The primary objective of this Note is to develop and test the basic modeling approach for equilibrium and near-equilibrium flows with pressure gradients.

Wall Region

The surface renewal model formulation for the mean flowfield near the wall of a steady two-dimensional uniform property turbulent boundary layer is given in terms of the mean burst frequency $\bar{s}$ by[2]

$$\frac{\partial \bar{u}}{\partial x}+\frac{\partial \bar{v}}{\partial y}=0 \tag{2}$$

$$\bar{s}(\bar{u}-\bar{U}_I)+\bar{u}\frac{\partial \bar{u}}{\partial x}+\bar{v}\frac{\partial \bar{u}}{\partial y}=\nu\frac{\partial^2 \bar{u}}{\partial y^2}-\frac{1}{\rho}\frac{\mathrm{d}\bar{P}}{\mathrm{d}x} \tag{3}$$

with $\bar{u}(0)=0$, $\bar{u}(y_M)=\bar{u}_M$, and $\bar{v}(0)=0$ for no transpiration; $\bar{U}_I$ represents the mean velocity within the large scale coherent structures at the first instant of inrush and $\bar{u}_M$ is the mean velocity at the interface between the wall region and the turbulent core. Strictly speaking, the inrush process carries fluid to within various small distances of the wall, such that U_I is random and nonuniform. However, for practical purposes, $\bar{U}_I$ can be approximated by a uniform initial velocity $\bar{U}_{Ic}$ for some applications. Setting $\bar{U}_I=\bar{U}_{Ic}$ and introducing the Couette flow approximation ($\partial\bar{u}/\partial x=0$) for adverse and mild-to-moderate favorable pressure gradients,

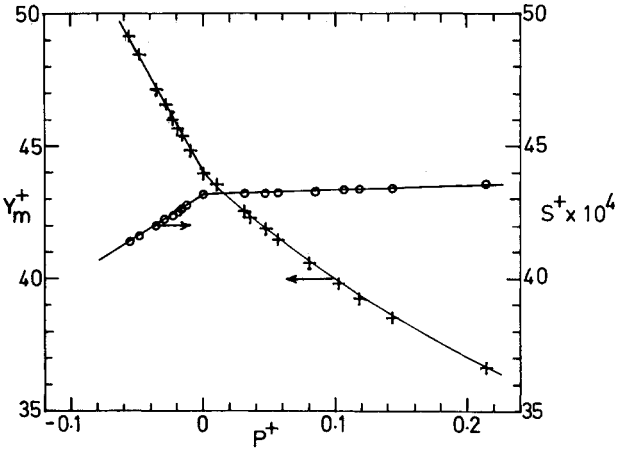

Fig. 1 Calculation for s^+ and y_M^+.

Eq. (3) reduces to

$$\bar{s}(\bar{u}-\bar{U}_{Ic})=\nu\frac{\mathrm{d}^2\bar{u}}{\mathrm{d}y^2}-\frac{1}{\rho}\frac{\mathrm{d}\bar{P}}{\mathrm{d}x} \tag{4}$$

Relaxing the constraint at the interface and requiring $\mathrm{d}\bar{u}/\mathrm{d}y=0$ as $y\to\infty$, the solution to Eq. (4) is

$$u^+=\left(U_{Ic}^+-\frac{P^+}{s^+}\right)[1-\exp(-y^+\sqrt{s^+})] \tag{5}$$

where

$$u^+=u/U^*,\quad U_{Ic}^+=\bar{U}_{Ic}/U^*,\quad y^+=yU^*/\nu$$

$$P^+=\frac{\nu}{U^{*3}}\frac{1}{\rho}\frac{\mathrm{d}\bar{P}}{\mathrm{d}x},\quad s^+=\frac{\nu\bar{s}}{U^{*2}}\ \text{and}\ U^*=\sqrt{\bar{\tau}_0/\rho}$$

Turbulent Core

The mixing-length approach is used to represent the mean transport within the turbulent core, with the familiar result

$$u^+=2\int_{y_M^+}^{y^+}\frac{1+P^+y^+}{1+\sqrt{1+4(\kappa y^+)^2(1+P^+y^+)}}\mathrm{d}y^+ + u_M^+ \tag{6}$$

Because of the range of applicability of the underlying Couette approximation, Eq. (6) applies throughout the intermediate region for adverse pressure gradients, but is restricted to smaller values of y^+ for favorable pressure gradients.

Closure

To close the analysis for the inner region, the wall modeling parameters s^+, U_{Ic}^+, u_M^+, and y_M^+ must be specified or evaluated. The modeling parameter U_{Ic}^+ can be expressed in terms of s^+ and P^+ by employing the Newton law of viscous shear at the wall (i.e., $\mathrm{d}u^+/\mathrm{d}y^+=1$ at $y^+=0$), with the result

$$U_{Ic}^+=\frac{1}{\sqrt{s^+}}+\frac{P^+}{s^+} \tag{7}$$

Combining Eqs. (5) and (7), the solution for u^+ becomes

$$u^+=\frac{1}{\sqrt{s^+}}[1-\exp(-y^+\sqrt{s^+})] \tag{8}$$

To express the modeling parameter y_M^+ in terms of s^+ and κ, the wall model is simply matched with the mixing-length formulation for the turbulent core by maintaining continuity in $\mathrm{d}u^+/\mathrm{d}y^+$. The resulting relation for y_M^+ is

$$\exp(-y_M^+\sqrt{s^+})=\frac{2(1+P^+y_M^+)}{1+\sqrt{1+4(\kappa y_M^+)^2(1+P^+y_M^+)}} \tag{9}$$

Setting $y^+=y_M^+$ in Eq. (8), u_M^+ is represented by

$$u_M^+=\frac{1}{\sqrt{s^+}}[1-\exp(-y_M^+\sqrt{s^+})] \tag{10}$$

With s^+ specified in terms of P^+ on the basis of experimental data, the values of U_{Ic}^+, y_M^+, and u_M^+ can be calculated by use of Eqs. (7), (9), and (10). Alternatively, following the approach generally employed in the establishment of the damping parameter a^+, s^+ can be calculated by using experimental data for u^+ within the inner region. Because of the lack of experimental measurements for mean frequency for boundary-layer flows with pressure gradients,

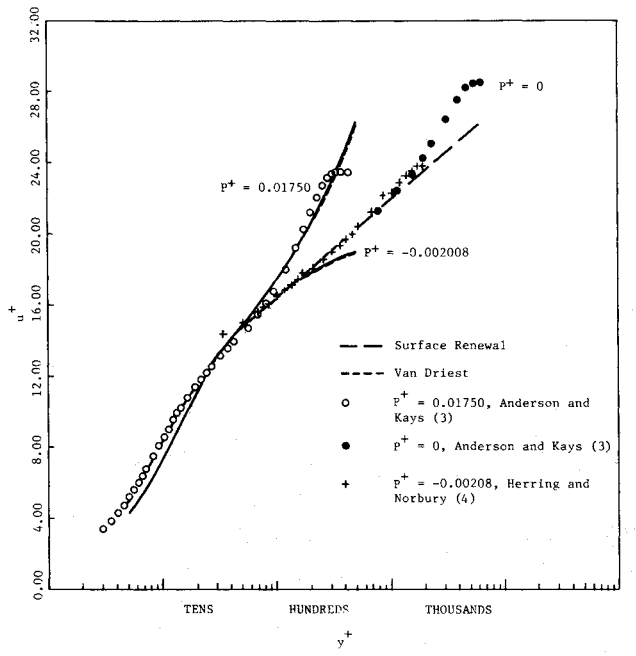

Fig. 2 Comparison of calculations for u^+ with experimental data.

the latter approach is used. Calculations obtained for s^+ and y_M^+ by coupling Eqs. (6) and (8) and matching the solution with representative experimental data[3] within the intermediate region are shown in Fig. 1. The analysis indicates a slight increase in s^+ and a moderate decrease in y_M^+ for increasing values of P^+ in the range $-0.01 \lesssim P^+ \lesssim 0.02$. The calculations for s^+ and y_M^+ are correlated to within 1% for $-0.01 \lesssim P^+ \lesssim 0.02$ by

$$s^+ = 0.004319(1 + aP^+) \tag{11}$$

where $a = 0.342$ for $P^+ > 0$ and $a = 7.5$ for $P^+ < 0$, and

$$y_M^+ = 44 - 910P^+, \qquad P^+ \leq 0 \tag{12a}$$

$$= 30 + 14\exp(-35P^+), \qquad P^+ \geq 0 \tag{12b}$$

Calculations for u^+ obtained using Eqs. (6) and (8-12) are compared with experimental data[3,4] in Fig. 2. Calculations obtained using the damping factor approach with a^+ specified as a function of P^+ by the correlation developed by Anderson et al.[3] are also shown in Fig. 2. The surface renewal and damping factor calculations for u^+ are essentially identical in the region for which $y^+ \gtrsim 20$. However, Eq. (8) lies moderately below the damping factor calculations and the experimental data for $y^+ \lesssim 20$, with a maximum difference of about 14% occurring at $y^+ = 7$. This difference, which is of no practical consequence in the analysis of the mean flowfield for turbulent boundary-layer flows, is primarily caused by the simplifying approximation $\bar{U}_I = \bar{U}_{Ic}$.

Conclusion

The present analysis demonstrates the usefulness of the surface renewal model for characterizing the wall region for fully turbulent boundary-layer flow with pressure gradients. The simple analytical relationship given by Eq. (8) expresses u^+ within the wall region in terms of the dimensionless burst frequency s^+ which is correlated in terms of P^+ by Eq. (11). When coupled with the classical mixing-length representation given by Eq. (6), the model predictions are essentially equivalent to results obtained by the damping factor method and are in good agreement with experimental data within the Couette flow region for adverse and favorable pressure gradients. The surface renewal inner law is readily incorporated into numerical codes by using Eq. (8) within the wall region, beginning the computational grid at y_M^+ and using the defining relations $u^+ = \bar{u}/U^*$ and $y^+ = yU^*/\nu$. The moderate underprediction of u^+ with the region $y^+ \lesssim 20$ is a result of the simplifying approximation $\bar{U}_I = \bar{U}_{Ic}$. Although the difference between Eq. (8) and the data in this region is of no practical consequence for this application, the effect of the unreplenished layer of fluid at the surface is significant for turbulent boundary-layer flows with blowing and heat and mass transfer. The more general surface rejuvenation model[5] provides a basis for analyzing these transport processes and for obtaining more accurate calculations within the close vicinity of the wall for pressure gradient flows.

Acknowledgment

Support provided for this study by the University of Petroleum and Minerals is gratefully acknowledged.

References

[1]van Driest, E. R., "On Turbulent Flow Near a Wall," *Journal of the Aeronautical Sciences*, Vol. 23, 1956, pp. 1007-1011.

[2]Thomas, L. C., "A Turbulence Burst Model of Wall Turbulence for Two-Dimensional Turbulent Boundary Layer Flow," *International Journal of Heat and Mass Transfer*, Vol. 25, 1982, pp. 1127-1136.

[3]Anderson, P. S., Kays, W. M., and Moffat, R. J., "Experimental Results for the Transpired Turbulent Boundary Layer in an Adverse Pressure Gradient," *Journal of Fluid Mechanics*, Vol. 69, 1975, pp. 353-375.

[4]Herring, H. and Norbury, J., "Some Experiments on Equilibrium Turbulent Boundary Layers in Favorable Pressure Gradients," *Journal of Fluid Mechanics*, Vol. 27, 1976, pp. 541-549.

[5]Thomas, L. C., "The Surface Rejuvenation Model of Wall Turbulence: Inner Laws for u^+ and T^+," *International Journal of Transfer*, Vol. 23, 1980, pp. 1097-1104.

Experimental Study of Surface Pressure in Three-Dimensional Turbulent Jet/Boundary Interaction

Christos D. Tsitouras* and Latif M. Jiji†
The City College of the City University of New York
New York, New York

Introduction

IT is well known that the presence of a boundary in the vicinity of a jet has a significant effect on the jet's behavior. Examples of jet/boundary interaction problems include impinging, wall, and offset jets. In the impinging jet, the fluid stream is directed toward a surface. In the wall jet, it is discharged parallel to and along a surface. In the offset jet, the fluid is discharged parallel to a surface from a nearby outlet (see Fig. 1). Clearly, the wall jet is a limiting case of the offset jet.

Although two-dimensional offset jets have been extensively investigated, little is known about three-dimensional offset jets. In this Note, we examine three-dimensional turbulent offset jets discharged from rectangular channels parallel to a

Received March 22, 1985; revision submitted Oct. 24, 1985.

*Graduate Student, Mechanical Engineering Department. Member AIAA.

†Herbert Kayser Professor, Mechanical Engineering Department. Member AIAA.